Veterinary Immunology and Immunopathology 209 (2019) 22–30

Contents lists available at ScienceDirect

Veterinary Immunology and Immunopathology

journal homepage: www.elsevier.com/locate/vetimm

Research paper

Molecular cloning and functional characterization of porcine 2′,5′-oligoadenylate synthetase 1b and its effect on infection with porcine reproductive and respiratory syndrome virus

Ruining Wang[a], Yinfeng Kang[b], Huawei Li[c], Hongfang Ma[d], Wenjia Wang[a], Yanfen Cheng[e], Pengchao Ji[d], Erqin Zhang[d], Mengmeng Zhao[d,*]

[a] School of Pharmaceutical Engineering, Henan University of Animal Husbandry and Economy, Zhengzhou 450046, People's Republic of China
[b] State Key Laboratory of Oncology in South China, Department of Experimental Research, Collaborative Innovation Center for Cancer Medicine, Sun Yat-sen University Cancer Center, Guangzhou 467500, People's Republic of China
[c] College of Biology Engineering, Henan University of Animal Husbandry and Economy, Zhengzhou 450046, People's Republic of China
[d] College of Animal Husbandry and Veterinary Medicine, Henan Agricultural University, Zhengzhou 450002, People's Republic of China
[e] College of Food Science and Engineering, Shanxi Agricultural University, Taigu 030801, People's Republic of China

ARTICLE INFO

Keywords:
PRRSV
OAS1b
RNase L
NTase
Replication

ABSTRACT

Porcine reproductive and respiratory syndrome virus (PRRSV) has previously been shown to increase porcine 2′-5′-oligoadenylate synthase (OAS) 1a expression, but the specific role of porcine OAS1b (pOAS1b) in PRRSV replication remains unknown. In this study, we conducted sequence analysis of the porcine *OAS1b* gene and studied the effects of its overexpression or silencing on PRRSV replication. OAS1b, localized mainly in the cytoplasm, was found to contain conserved protein domains, such as the P-Loop and D-Box, indicating that its nucleotidyl transferase activity was complete and the antiviral effect depended on ribonuclease L (RNase L). OAS1b overexpression inhibited PRRSV replication, whereas small-interfering-RNA silencing of *OAS1b* resulted in increased virus titers. Additionally, OAS1b promoted expression of interferons as well as interferon-β promoter activity. These results lay the theoretical foundation for the development of new anti-PRRSV strategies.

1. Introduction

Innate immunity is the first line of defense against invasion of foreign objects or pathogens. When molecules with pathogen-associated molecular patterns invade the body, they are recognized and activate a number of pattern recognition receptors to induce interferon and interleukin secretion (Schoggins et al., 2015). These cytokines next promote the secretion of related antiviral molecules, such as 2′,5′-oligoadenylate synthase (OAS), myxovirus resistance A (Mx), and protein kinases, which then go on to exert their antiviral effects (Hovanessian, 2007; Hovanessian and Justesen, 2007). OAS was first discovered in human cells in 1974 (Hovanessian and Kerr, 1979) and was then gradually found in many other species (Shimizu and Sokawa, 1983). The OAS family of enzymes plays an important role in many cellular processes, such as apoptosis, cell differentiation, and immunity (Chebath et al., 1987; Sokawa and Sokawa, 1986; Tessier et al., 2006; Triozzi et al., 1989). OAS activates ribonuclease L, which degrades both cellular and viral RNAs (Cagliani et al., 2012; Castelli et al., 1998; Dong and Silverman, 1997).

Human OASs include OAS1, OAS2, OAS3, and 2′,5′-oligoadenylate synthase–like protein (OASL) (Eskildsen et al., 2003; Hartmann et al., 2003, 1998; Hovanessian and Justesen, 2007; Kakuta et al., 2002). The porcine OAS family consists of OAS1, OAS2, and OASL. Porcine OAS1 and OASL have one OAS domain each, whereas OAS2 possesses two OAS domains. In the *OASL* gene, there is a stop codon that results in the early termination of translation of its mRNA.

Porcine reproductive and respiratory syndrome is a highly contagious and infectious disease caused by porcine reproductive and respiratory syndrome virus (PRRSV). The virus was discovered in the United States of America (Benfield et al., 1992) and then spread globally, causing great economic losses and becoming the number one enemy of pig industries worldwide. The disease was first reported in China in 1996, and a 2006 outbreak of a new highly virulent PRRSV strain—having a 30–amino acid deletion in its nonstructural protein (NSP) 2 region—had a particularly devastating impact on the local pig industry (Tian et al., 2007). Since then, PRRSV has undergone

* Corresponding author.
E-mail address: zhaomengmeng2016@outlook.com (M. Zhao).

https://doi.org/10.1016/j.vetimm.2019.01.003
Received 23 July 2018; Received in revised form 10 January 2019; Accepted 21 January 2019

continuous recombination and mutation under various types of immune pressure in China. In 2010, another new strain appeared for which there was no effective drug (Zhou et al., 2015). Therefore, the development of a new antivirus strategy has become a top priority.

PRRSV is a positive-sense, single-stranded RNA virus belonging to the family *Arteriviridae* (order *Nidovirales*) (Cavanagh, 1997). The PRRSV genome contains 10 open reading frames (ORFs), among which ORF7 encodes the nucleocapsid (N) protein. Some of the few cell types that are known to be susceptible to this virus are porcine alveolar macrophages (PAMs) (Kim et al., 1993) and the monkey-derived Marc-145 cell line (Benfield et al., 1992).

Proteomic studies have revealed that PRRSV infection causes an increase in OAS protein levels in PAMs (Li et al., 2017a), but the exact mechanism behind this effect is unknown. Although the antiviral effect of porcine OAS1a (pOAS1a) has been tested (Zhao et al., 2016a), that of porcine OAS1b (pOAS1b) and its mechanism of action are unknown. Therefore, we cloned the *OAS1b* gene from Chinese domestic pigs and verified its antiviral effect on PRRSV. Our results should provide a theoretical basis for exploring the immune characteristics of pOAS1b as well as for prevention and treatment of PRRSV infection.

2. Materials and methods

2.1. Cells and viruses

Porcine alveolar macrophages (PAMs), isolated from lung lavage fluids of 7-week-old pigs that were free of PRRSV, of pseudorabies virus, of type 2 porcine circovirus, and of classical swine fever virus, were cultured in Roswell Park Memorial Institute (RPMI; Invitrogen, Carlsbad, CA, USA) 1640 medium supplemented with 10% of fetal bovine serum (Life Technologies, Carlsbad, CA, USA) at 37 ℃ in a humidified atmosphere containing 5% of CO_2.

CRL-2843-CD163, a stable porcine macrophage cell line that carries the CD163 receptor and thus can be infected by PRRSV (Zhao et al., 2017a), was kindly provided by Prof. Enmin Zhou (Northwest A&F University, Lingyang, China). They were grown in the RPMI 1640 medium with 6% of fetal calf serum (Invitrogen, Carlsbad, CA, USA) at 37 ˚C and 5% CO_2; Marc-145 cells were cultured in Dulbecco's Modified Eagle's Medium (DMEM; Invitrogen, Carlsbad, CA, USA) supplemented with 10% of fetal calf serum (Sijiqing, ZhejiangTianhang Biotechnology Co. Ltd., China) at 37 ˚C and 5% CO_2, and type 2 PRRSV (XH-GD strain) (GenBank accession No. EU624117) was maintained in the laboratory (Wang et al., 2018b).

2.2. RNA extraction and reverse transcription

RNA from different groups of PAMs and CRL-2843-CD163 cells was extracted using the TRIzol Reagent (Invitrogen, Carlsbad, CA, USA), and reverse transcription was performed with the PrimeScript First Strand cDNA Synthesis Kit (Takara, Dalian, China).

2.3. OAS1b cloning

After the reverse transcription was completed, the cDNA was used as a template for polymerase chain reaction (PCR) amplification with primers OAS1b-F and OAS1b-R (Table 1) and the LA Taq enzyme (Takara, Dalian, China). The PCR product was digested and ligated to the pCMV-3xFLAG-7.1 vector (Sigma-Aldrich, St. Louis, MO, USA), and the construct was verified by sequencing. The Mix & Go! *E. coli* Transformation Kit (Zymo Research, USA) was used for transformation.

2.4. Sequence alignment and sequence analysis

The ClustalW software was employed to compare the DNA and protein sequences among different species, and MEGA 4.0 software was used to build a phylogenetic tree as described previously (Zhao et al., 2013). The main biological characteristics of the OAS1b protein were predicted by means of the ProtParam tool (available on the website http://web.expasy.org/protparam/); we determined the amino acid sequence length, isoelectric point, molecular weight, and molecular formula. The Network Protein Sequence @nalysis web server was employed to construct a pattern map and to determine the secondary structure (https://npsa-prabi.ibcp.fr/cgi-bin/npsa_automat.pl?page=/NPSA/npsa_sopma.html). DNASTAR package version 7.0 (DNASTAR, Madison, WI, USA) was used to predict the protein's antigenicity and the amino acid sequence similarities among different species. STRING (http://string-db.org/cgi/input.pl?UserId=8AG3IJsO1vO1&sessionId=CqlMDWa9qxEm&input_page_active_form=single_identifier) served to predict the proteins that would interact with OAS1. SWISS-MODEL (https://swissmodel.expasy.org/) was employed to calculate the tertiary structure of the protein. Phosphorylation sites of the protein were predicted by NetPhos-3.1 (http://www.cbs.dtu.dk/services/NetPhos-3.1/), glycosylation sites were predicted by NetNGlyc 1.0 (http://www.cbs.dtu.dk/services/NetNGlyc/), signal peptides by SignalP 4.1 (http://www.cbs.dtu.dk/services/SignalP/), transmembrane domains by TMHMM version 2.0 (http://www.cbs.dtu.dk/services/TMHMM/), and the protein's hydrophilicity was evaluated by ProtSCale (http://web.expasy.org/protscale/). The subcellular localization of pOAS1b was predicted in the PSORT software (https://psort.hgc.jp/form2.html). Finally, its function was predicted by means of ProtFun 2.2 (http://www.cbs.dtu.dk/services/ProtFun/).

Table 1
Primers used in the research.

Primer	Sequence
OAS1b- For	CTAGCTAGCGCCACCATGGATACCCCTGTTAGGGAC
OAS1b- Rev	CCGCTCGAGTCAGATATCTTCCTCCTGTGGAG
qOAS1b-F	CGGAAATCTACGTCCAGCTT
qOAS1b-R	GCTCTTCAGCTTGGTTGGTC
qGAPDH-F	CTGCCGCCTGGAGAAACCT
qGAPDH-R	GCTGTAGCCAAATTCATTGTCG
Si-OAS1b	GGCACAUGAGCGUUUCCAUTT
	AUGGAAACGCUCAUGUGCCTT
Si-RIG-I	GCCCUUAACCAAGCAGGUUTT
	AACCUGCUUGGUUAAGGGCTT
Si-RNase L	UGGAAGAGAUGAAUGCAUATT
	UAUGCAUUCAUCUCUUCCATT
Si-MDA5	CCGAAGGAUUGAUGCCUAUTT
	AUAGGAUCAAUCCUUCGGTT
Si-IRF3	GCUGAUAUCUCAGCUGUUCCUTT
	UGGUUCAGCUGAGAUAUCAGCTT
qIRF3-F	AAGGTTGTCCCCATGTGTCTCCG
qIRF3-R	GGAAATGTGCAGGTCCACCGTG
qIRF7-F	TCCAGCCGAGATGCTAAGTG
qIRF7-R	GTCCAAGTCCTGCCCGATGT
qN-F	AAACCAGTCCAGAGGCAAGG
qN-R	GCAAACTAAACTCCACAGTGTAA
qIFN-beta -F	CTAGCACTGGCTGGAATGAGACT
qIFN-beta -R	GGCCTTCAGGTAATGCAGAATC
qTNF-alpha-F	CACCACGCTCTTCTGCCTAC
qTNF-alpha-R	ACGGGCTTATCTGAGGTTTGAG
qIL-8-F	GGCAGTTTTCCTGCTTTCT
qIL-8-R	CAGTGGGGTCCACTCTCAAT
qRIG-I-F	CAGAGCAGCGGCGGAATC
qRIG-I-R	ACTCAAGGTTGCCCAT
qTLR7-F	GAACTGTTTC TCTACAACA
qTLR7-R	AGACTTGTAATTCTGTCA
qTLR3-F	TACTGTACAC AACTTCTACC
qTLR3-R	TTAAATCCTCCATCCAAGG
qNF-κB-F	CCAGCACCTCCACTCCATTC
qNF-κB-R	ACATCAGCACCCAAAGACACC
qMDA5-F	CGAATTAACAGGCACCGATT
qMDA5-R	CGTCCAGACTTGGCTGATCT
qMyD88-F	CTCCGGAGCG GAGTCCGCG
qMyD88-R	GCCAGCCCAGTCCAGTCC
qTBK1-F	CCAGTGGAT GTTCAAAT
qTBK1-R	CTCCCACATGGACAAAAT

2.5. Tissue distribution

All Pigs were sacrificed using euthanasia approved by the Ethical Committee of Henan Agricultural University. Samples of heart, liver, spleen, kidneys, brain, intestine, and lymph nodes are frozen in liquid nitrogen, lungs were removed for lavage. RNA was extracted from different pig organs (the heart, liver, spleen, kidneys, brain, intestine, and lymph nodes), and reverse transcription was performed. The distribution of OAS1b among the different organs was determined by quantitative polymerase chain reaction (qPCR) analysis.

2.6. Effects of different stimuli on OAS1b

PAMs grown in a 24-well plate at over 90% confluence were infected with the PRRSV XH-GD strain at multiplicity of infection (MOI) of 0.1, and the cells were collected at different time points (0, 6, 12, 24, 36, and 48 h). The mRNA expression of *OAS1b* was detected by qPCR. PAMs at over 90% confluence grown in a 24-well plate were stimulated with interferon (IFN) β (Sigma-Aldrich) at a dose of 1000 IU/mL and then were harvested at different time points (0, 6, 12, 24, 36, and 48 h). The mRNA expression of *OAS1b* was assessed by qPCR. PAMs at over 90% confluence grown in a 24-well plate were stimulated with Poly (I:C) (Sigma-Aldrich) at a dose of 1.5 μg/mL, and the cells were harvested at different time points (0, 2, and 4 h). The mRNA expression of *OAS1b* was determined by qPCR. PAMs at over 90% confluence grown in a 24-well plate were stimulated with lipopolysaccharide (LPS; Sigma-Aldrich) at a dose of 15 μg/mL, and the cells were collected at different time points (0, 2, and 4 h). The mRNA expression of *OAS1b* was determined by qPCR.

2.7. Small interfering RNA (siRNA)

SiRNAs were designed to target *OAS1b*, *RNase L*, *RIG-I*, and *MDA5* (sequences are provided in Table 1). The siRNAs were synthesized by GenePharma Co., Ltd. (Suzhou, China).

2.8. Transfection

PAMs or CRL-2843-CD163 cells were grown to confluence of 70% in a 24-well plate and then transfected with either 60 nM of siRNA or 500 ng of pCMV-3xFLAG-7.1 (control vector) or pCMV-3xFLAG-7.1-OAS1b vector. All transfections were performed by means of Lipofectamine 3000 (Invitrogen).

2.9. An indirect immunofluorescence assay (IFA)

CRL-2843-CD163 cells grown at 70% confluence in a 24-well plate were transfected with 500 ng of the control vector or pCMV-3xFLAG-7.1-OAS1b vector. After 24 h, the IFA was performed as described previously (Zhao et al., 2016b) with an anti-FLAG monoclonal antibody (1:50; Abbkine Wuhan, China) as the primary antibody, and a fluorescein-5-isothiocyanate (FITC)-labeled anti-rabbit IgG antibody (1:100; Beijing Biosynthesis Biotech Co., Ltd., China) as the secondary antibody (Zhao et al., 2016b).

2.10. A cytotoxicity assay

Enhanced Cell Counting Kit-8 (Beyotime Biotech, Shanghai, China) was used to test the toxicity of pOAS1b and of the transfected vectors and siRNA toward PAMs and CRL-2843-CD163 cells.

2.11. qPCR

The mRNA expression levels of IFN-α, IFN-β, interleukin (IL)-8, IL-1β, interferon regulatory factor (IRF) 3, IRF7, Toll-like receptor (TLR) 3, TLR7, retinoic-acid–inducible gene I (RIG-I), melanoma differentiation–associated protein 5 (MDA5), myeloid differentiation primary response 88 (MyD88), TANK-binding kinase 1 (TBK1), and nuclear factor kappa B (NF-κB) were determined by qPCR. *GAPDH* served as an internal reference, and relative changes in expression of the target genes were calculated via the $2^{-\triangle\triangle Ct}$ formula, and the primer sequences are given in Table 1.

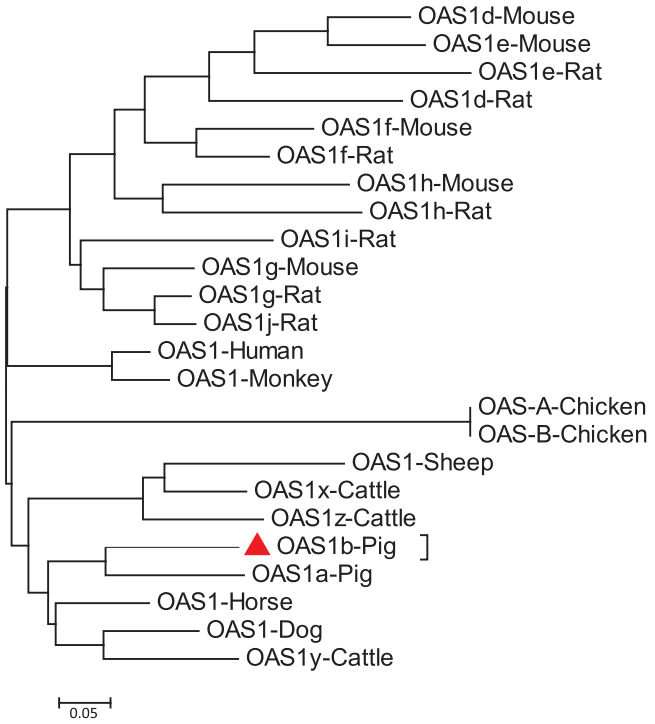

Fig. 1. Comparison of the OAS1b sequence from pigs with that from other species.
Phylogenetic analysis of OAS1 from different species: pig OAS1a (GenBank accession No. MG799562), pig OAS1b (MG799560), human OAS1 (NM_016816), horse OAS1 (AY321355), mouse OAS1a (NM_145211), mouse OAS1b (AF328926), mouse OAS1f (NM_145153), mouse OAS1h (NM_145228), rat OAS1d (NM_001009379), rat OAS1f (NM_001009490), rat OAS1h (NM_001009491), rat OAS1i (NM_001009680), chicken OAS*A (KU058695), chicken OAS*B (NP_990372), cattle OAS1x (NM_178108), cattle OAS1y (AY243505), and cattle OAS1z (NM_001029846).

2.12. Western blotting

After PRRSV infection or IFN stimulation of PAMs, western blotting was performed to determine the OAS1b protein levels in the cells, with anti-OAS1b as the primary antibody (1:100; Abcam, Massachusetts, CT, USA).

For the evaluation of pOAS1b overexpression by western blotting, the primary antibodies were anti-FLAG (1:200; Abnova, Taipei, Taiwan) and anti-GAPDH (1:1000; Beijing Biosynthesis Biotech Co., Ltd., Beijing, China), and the secondary antibodies were a horseradish peroxide (HRP)-conjugated goat anti-rabbit IgG antibody (1:10,000; Zhongshan Golden bridge Biotechnology, Beijing, China) and an HRP-conjugated goat anti-mouse IgG antibody (1:10,000; Jackson ImmunoResearch, West Grove, PA, USA). To determine the amount of phosphorylated IRF3 (p-IRF3), anti-p-IRF3 (1:1000; Cell Signaling Technology, Danvers, MA, USA) and anti-IRF3 (1:200; Santa Cruz, USA) antibodies were employed as described before (Wang et al., 2018a).

2.13. The tissue culture 50% infectious dose ($TCID_{50}$)

The supernatant of virus-infected cell cultures was collected for determination of the virus titer on Marc-145 cells. The virus titer was

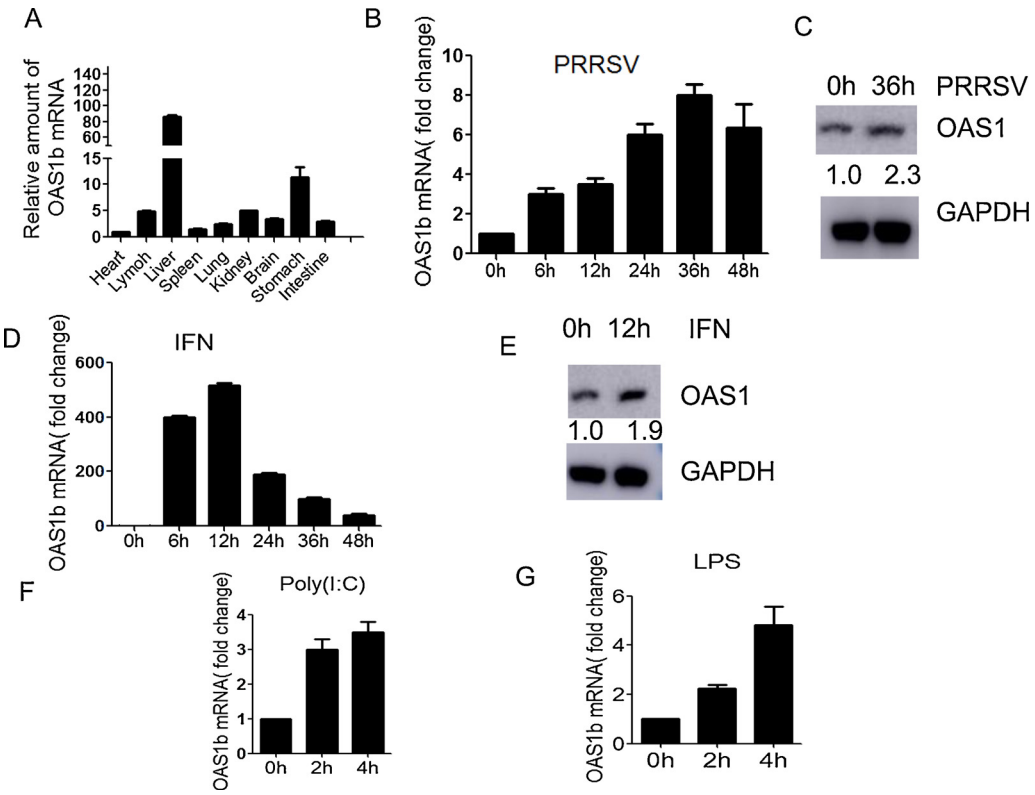

Fig. 2. Changes of pOAS1b expression in porcine alveolar macrophages (PAMs) and tissue distribution after different stimuli.

(A) Distribution of *OAS1b* mRNA in various pig organs, as determined by qPCR. *GAPDH* served as a control gene. The following organs were analyzed: the heart, lymph nodes, liver, spleen, lung, kidneys, brain, stomach, and intestine. Data represent means ± s.d. of three independent experiments, relative changes in expression of the target genes were calculated via the $2^{-\triangle\triangle Ct}$ formula.

(B) PRRSV infection activates OAS1b expression. PAMs at over 90% confluence grown in a 24-well plate were infected with PRRSV at MOI 0.1 and then harvested at different time points (0, 6, 12, 24, 36, and 48 h) for qPCR analysis of *OAS1b* mRNA. *GAPDH* was used as a control gene. Relative amounts of *OAS1b* mRNA were compared with those in the 0 h sample. Error bars represent SD.

(C) Western blotting analysis of OAS1b expression at 36 h postinfection (h.p.i.) with PRRSV. PAMs at over 90% confluence grown in a 24-well plate were infected with PRRSV at MOI 0.1 and then harvested at 36 h.p.i.; after that, the cells were subjected to western blotting. Anti-OAS1b (Abcam, 1:1000, USA) served as the primary antibody, GAPDH was used as the internal reference.

(D) Treatment with IFN activates *OAS1b* expression. PAMs at over 90% confluence grown in a 24-well plate were treated with 1000 IU/mL IFN-β and then harvested at different time points (0, 6, 12, 24, 36, and 48 h) for qPCR quantitation of *OAS1b* mRNA; *GAPDH* served as a control gene.

(E) Western blotting of OAS1b expression after 12 h of IFN-β treatment. PAMs at over 90% confluence grown in a 24-well plate were infected with PRRSV at MOI 0.1 and then were harvested at 36 h.p.i. and subjected to western blotting. Anti-OAS1b (Abcam, 1:1000, USA) served as the primary antibody, and GAPDH was used as the internal reference.

(F) Poly(I:C) activates *OAS1b* expression. PAMs at over 90% confluence grown in a 24-well plate were incubated with 1.5 μg/mL Poly(I:C) and then harvested at different time points (0, 2, and 4 h) for qPCR measurement of *OAS1b* mRNA expression; *GAPDH* served as a control gene.

(G) LPS activates *OAS1b* expression. PAMs at over 90% confluence grown in a 24-well plate were treated with 15 μg/mL LPS and then harvested at different time points (0, 2, and 4 h) for qPCR measurement of *OAS1b* mRNA expression; *GAPDH* served as a control gene.

expressed as the $TCID_{50}$.

2.14. An ELISA

An ELISA kit (Cloud-Clone Group, USA) was employed to measure the porcine IFN-β levels in the cells.

2.15. A luciferase reporter assay

Cells at 70% confluence in a 24-well plate were transfected with 500 ng of the control vector or pCMV-3xFLAG-7.1-OAS1b vector, 200 ng of the IFN-β-Luc reporter plasmid, and 50 ng of pRL-TK. After 24 h of incubation, the luciferase reporter assay was performed as described elsewhere (Fu et al., 2017).

2.16. Statistical analysis

Each experiment was repeated three times with three technical replicates each time. Differences between groups were considered statistically significant at $P < 0.05$ and < 0.01.

3. Results

3.1. Sequence alignment and analysis of OAS1b

Comparison of the pig OAS1 sequences with OAS1 sequences of other species revealed that they contain multiple conserved regions, such as the P-loop and D-box domain. Nonetheless, there was no ubiquitinlike (UBL) domain in pOAS1b (Supplementary materials, Fig. S1). Phylogenetic-tree analysis showed that pig *OAS1b* is located in the same branch as cattle and horse *OAS1*s, with relatively close genetic evolution (Fig. 1). Sequence analysis indicated that the full-length coding sequence of porcine OAS1b is 1068 bp in size, encoding 355 amino acid residues. The protein's molecular formula is $C_{1848}H_{2876}N_{490}O_{528}S_{10}$, with a molecular weight of 40,726. Its instability value turned out to be 40.93, indicating that it is an unstable protein, with a half-life of 30 h. Its isoelectric point is 8.45. A model map created according to the amino acid sequence comparison results is presented in Supplementary materials, Fig. S2A. The secondary structure analysis of OAS1b revealed that it consists of 41.69% of α-helices and of 35.49% of random coils (Supplementary materials, Fig. S2B). Within the protein, there are multiple regions with highly antigenic sites (Supplementary materials, Fig. S2C). STRING analysis revealed that OAS1b interacts with ubiquitin-specific protease 43 (USP43); proteasome 26S subunit; non-ATPase 4; ribosomal proteins S27A, S4, and S3 A; RAB guanine nucleotide exchange factor 1; and other proteins (Supplementary materials, Fig. S2D). Amino acid similarity analysis revealed that the similarity of pOAS1b and pOAS1a to those of other species varied from 50.0% to 87.9% (Supplementary materials, Fig. S2E). The tertiary structure of pOAS1b was predicted to be similar to that of pOAS1a but distant from the structure of other OAS1 proteins (Supplementary materials, Fig. S2F). NetPhos-3.1 predicted phosphorylation of 17 serine sites, 21

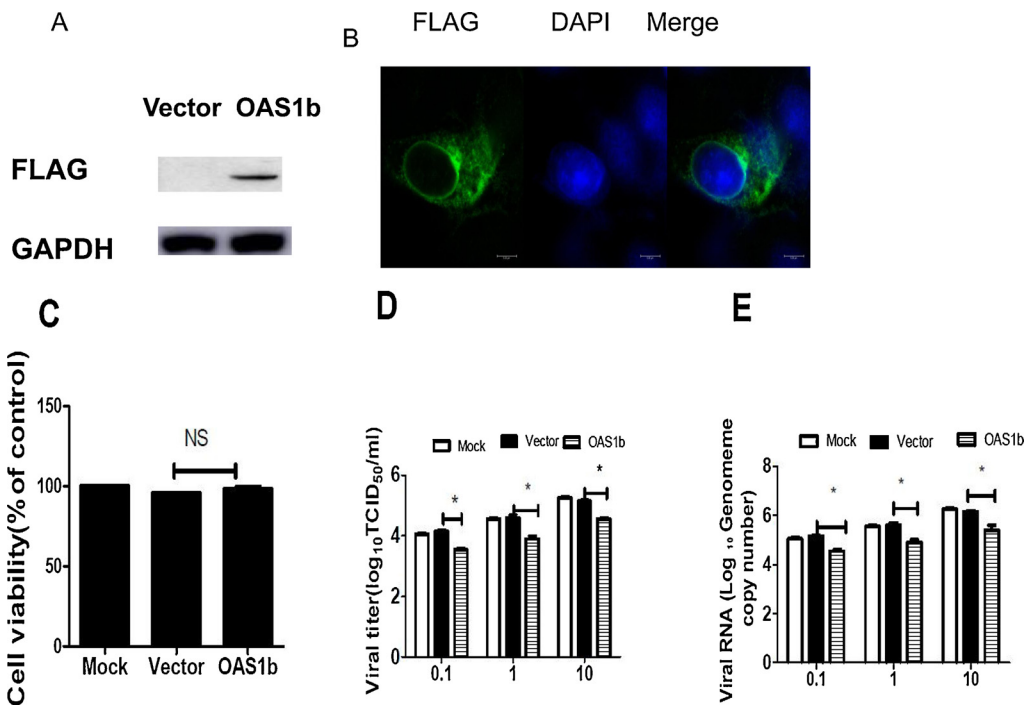

Fig. 3. pOAS1b overexpression inhibits PRRSV replication.
(A) pOAS1b was overexpressed in CRL-2843-CD163 cells. Western blotting analysis of pOAS1b expression in cells transfected with either 500 ng of OAS1b-carrying vector or a control vector for 48 h. Anti-FLAG was used as the primary antibody, and GAPDH as the internal reference.
(B) An indirect immunofluorescent assay (IFA) for the subcellular localization of pOAS1b. In brief, 500 ng of the FLAG-tagged OAS1b plasmid was transfected into CRL-2843-CD163 cells for 24 h; the cells were fixed with cold methanol and incubated with an anti-FLAG antibody.
(C) Viability of CRL-2843-CD163 cells transfected with either 500 ng of the FLAG-tagged OAS1b–expressing vector or a control vector for 48 h. The Enhanced Cell Counting Kit-8 (Beyotime Biotech, Shanghai, China) was employed to test the toxicity.
(D) CRL-2843-CD163 cells were transfected with 500 ng of pCMV-3xFLAG-7.1-pOAS1b or pCMV-3xFLAG-7.1; at 24 h later, the cells were infected with PRRSV at the indicated MOI, and after 48 h, virus titers were determined as $TCID_{50}$ in Marc-145 cells. All the experiments involved three biological replicates.
(E) qPCR analysis of PRRSV N mRNA copy number in CRL-2843-CD163 cells transfected with either the OAS1b-carrying vector or control vector and then were infected with the virus at different MOI (0.1, 1, or 10).

threonine sites, and 10 tyrosine sites (Supplementary materials, Fig. S3A). TMHMM Server v. 2.0 did not detect transmembrane regions in OAS1b (Supplementary materials, Fig. S3B). The SignalP 4.1 Server did not detect any signal peptides in this protein either (Supplementary materials, Fig. S3C). ProtSCale predicted that there were many hydrophilic regions, indicating that OAS1b is a hydrophilic protein (Supplementary materials, Fig. S3D). PSORT predicted that 39.1% of OAS1b is located in the cytoplasm, 39.1% in the nucleus, and 17.4% in mitochondria. The ProtFun 2.2 server predicted that this protein belongs to the functional categories of transport and binding, cell envelope, and voltage gated ion channel and appeared to be a transferase.

3.2. Organ distribution of OAS1b mRNA

OAS1b mRNA was found to be present in all the organs tested, but its amounts in the liver and stomach were the highest (Fig. 2A).

3.3. Effects of different stimuli on OAS1b

After PRRSV infection, the expression of *OAS1b* mRNA increased continuously, reaching the highest level at 36 h, where it was ˜8-fold higher than that in the no-treatment control (Fig. 2B). This result was confirmed by the western blotting data, indicating elevated OAS1b protein levels at 36 h post infection (Fig. 2C). After stimulation with IFN-beta, the expression of *OAS1b* mRNA increased continuously, reaching the highest level at 12 h, where it was approximately 500-fold higher than that in the no-treatment control (Fig. 2D). This was confirmed by the western blotting results at 12 h post-treatment (Fig. 2E).

After stimulation with Poly(I:C), the expression of *OAS1b* mRNA increased continuously, reaching the highest level at 4 h, where it was ˜3.5-fold higher relative to the no-treatment control (Fig. 2F). After stimulation with LPS, the expression of *OAS1b* mRNA increased continuously, reaching the highest level at 4 h, where it was ˜4.5-fold higher relative to the no-treatment control level (Fig. 2G).

3.4. The effect of pOAS1b overexpression on PRRSV replication

pOAS1b was efficiently expressed in the CRL-2843-CD163 cells, as demonstrated by the western blotting results (Fig. 3A). According to the IFA results, green fluorescence was concentrated mainly in the cytosol (Fig. 3B). the percentage of transfection efficiency was 60%. The cell viability assay results suggested that pOAS1b is not significantly toxic to the cells (Fig. 3C).

Twenty-four hours after OAS1b transfection, different doses of PRRSV (MOI 0.1, 1, or 10) were inoculated, and after another 48 h, qPCR and $TCID_{50}$ were used to evaluate replication of the virus.

The qPCR results showed that the PRRSV N mRNA copy number decreased (Fig. 3D); this finding was verified by the virus titer assay, which indicated that $TCID_{50}$ for the pOAS1b-overexpressing cells decreased significantly (Fig. 3E).

3.5. Effects of pOAS1b overexpression on IFN and related signaling factors

After pOAS1b overexpression, the mRNA levels of IFN-α and IFN-β significantly increased, whereas those of IL-1β, IL-8, and TNF-α did not change significantly relative to the cytokine levels in the control vector–transfected cells (Fig. 4A). Some factors of relevant pathways were also upregulated to varying degrees (Fig. 4B).

The ELISA results suggested that the level of IFN-β increased after pOAS1b overexpression (Fig. 4C). Western blotting indicated that the amount of p-IRF3 also went up (Fig. 4D), and the activity of the IFN-β promoter obviously increased after stimulation by PRRSV or Poly(I:C) (Fig. 4E).

3.6. The influence of OAS1b silencing on PRRSV replication

The qPCR results showed that *OAS1b* mRNA was effectively knocked down after si-OAS1b was transfected into PAMs (Fig. 5A). After inoculation with PRRSV at MOI 0.1, both the virus titer and PRRSV N mRNA copy number significantly increased (Fig. 5B, 5C). In

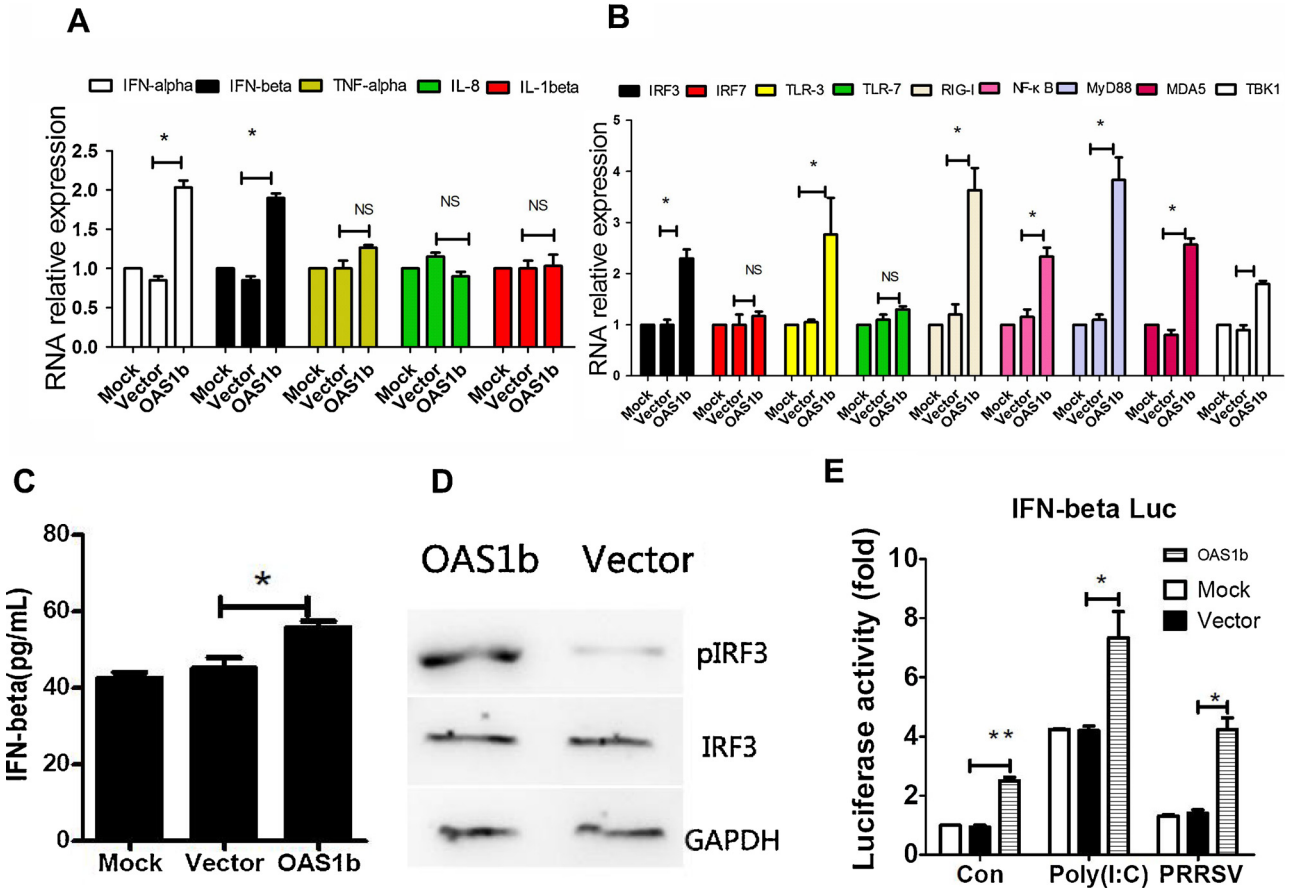

Fig. 4. pOAS1b overexpression activates proteins of various relevant pathways. (A) qPCR measurement of the mRNA expression of different cytokines (IFN-α, IFN-β, IL-8, IL-1β, and TNF-α) in pCMV-3xFLAG-7.1-OAS1b–transfected CRL-2843-CD163 cells. (B) qPCR measurement of the mRNA expression of factors of different pathways in the OAS1b-overexpressing cells. (C) An ELISA of the IFN-β protein level in the OAS1b-overexpressing cells. (D) A western blot of the p-IRF3 protein levels in the OAS1b-overexpressing cells. (E) A luciferase reporter assay of the IFN-β promoter activity in the OAS1b-overexpressing cells.

another experiment, the mRNA expression of IFN-β was determined by qPCR after Poly(I:C) stimulation of the siRNA-transfected cells (Fig. 5D); the results uncovered a decrease in the IFN-β mRNA level in the si-OAS1b–transfected cells. Cell viability assays suggested that si-OAS1b is nontoxic to PAMs (Fig. 5E).

3.7. The effect of RNase l silencing on PRRSV replication

The qPCR results revealed that RNase L was effectively knocked down after transfection of si-RNase L into PAMs (Fig. 5F). After the knockdown, there was no significant change in the virus titer and PRRSV N mRNA copy numbers (Fig. 5G and H). The cell viability assays suggested that si-RNase L was not toxic to PAMs (Fig. 5I).

3.8. The influence of RIG-I and MDA5 silencing on PRRSV replication

In PAMs transfected with siRNAs directed against *RIG-I*, its mRNA expression was knocked down by approximately 60% (Fig. 6A). To determine whether RIG-I is required for anti-PRRSV activity, cells were cotransfected with si-RIG-I and si-OAS1b and then infected with PRRSV at MOI 0.1. After 24 h, virus replication was determined by $TCID_{50}$ measurement and via the N mRNA copy numbers (by qPCR). The results revealed that there was still a significant increase in $TCID_{50}$ and an increase in PRRSV N mRNA copy numbers in the knockdown cells relative to control cells after cotransfection with si-RIG-I and si-OAS1b (Fig. 6B, C).

Likewise, siRNAs targeting *MDA5* were transfected into PAMs, and after 24 h, these siRNAs knocked the *MDA5* mRNA expression down by approximately 55% (Fig. 6D). After cotransfection of the cells with si-MDA5 and si-OAS1b, and PRRSV (0.1 MOI) infection 24 h later, the virus replication status was determined by $TCID_{50}$ measurement and by qPCR (evaluating PRRSV N mRNA copy numbers). The results showed that there were still significant differences in $TCID_{50}$ values (Fig. 6E) and N mRNA expression (Fig. 6F) between the knockdown and control cells. Thus, the antiviral effect was found to be independent of RIG-I and MDA5.

4. Discussion

Pattern recognition receptors are used by innate immunity for defense against external-pathogen invasion. TLRs and RIG-I–like receptors have been characterized and found to be pattern recognition receptors. They sense viral nucleic acids and inhibit viral infection by activating expression of type I IFN. The latter activates hundreds of IFN-stimulated genes, which in turn inhibit viral infection. IFN-stimulated genes mainly include OAS, Mx, ISG50, ISG15, and interferon-induced transmembrane proteins (IFITMs). By contrast, innate immunity impairs viral infection by direct interaction between host factors and the virus (Patil et al., 2018). It has been reported that porcine Mx inhibits PRRSV replication by interacting with the PRRSV N protein (Wang et al., 2016). Several OAS proteins have been reported to be intrinsic restriction factors (Fu et al., 2017; Yang et al., 2016; Zhao et al., 2017a,b); similarly, our study indicates that pOAS1b directly suppresses viral infection. Thus, pOAS1b is an intrinsic immune factor that inhibits PRRSV infection.

In this study, pOAS1b was cloned, and the results of its sequence

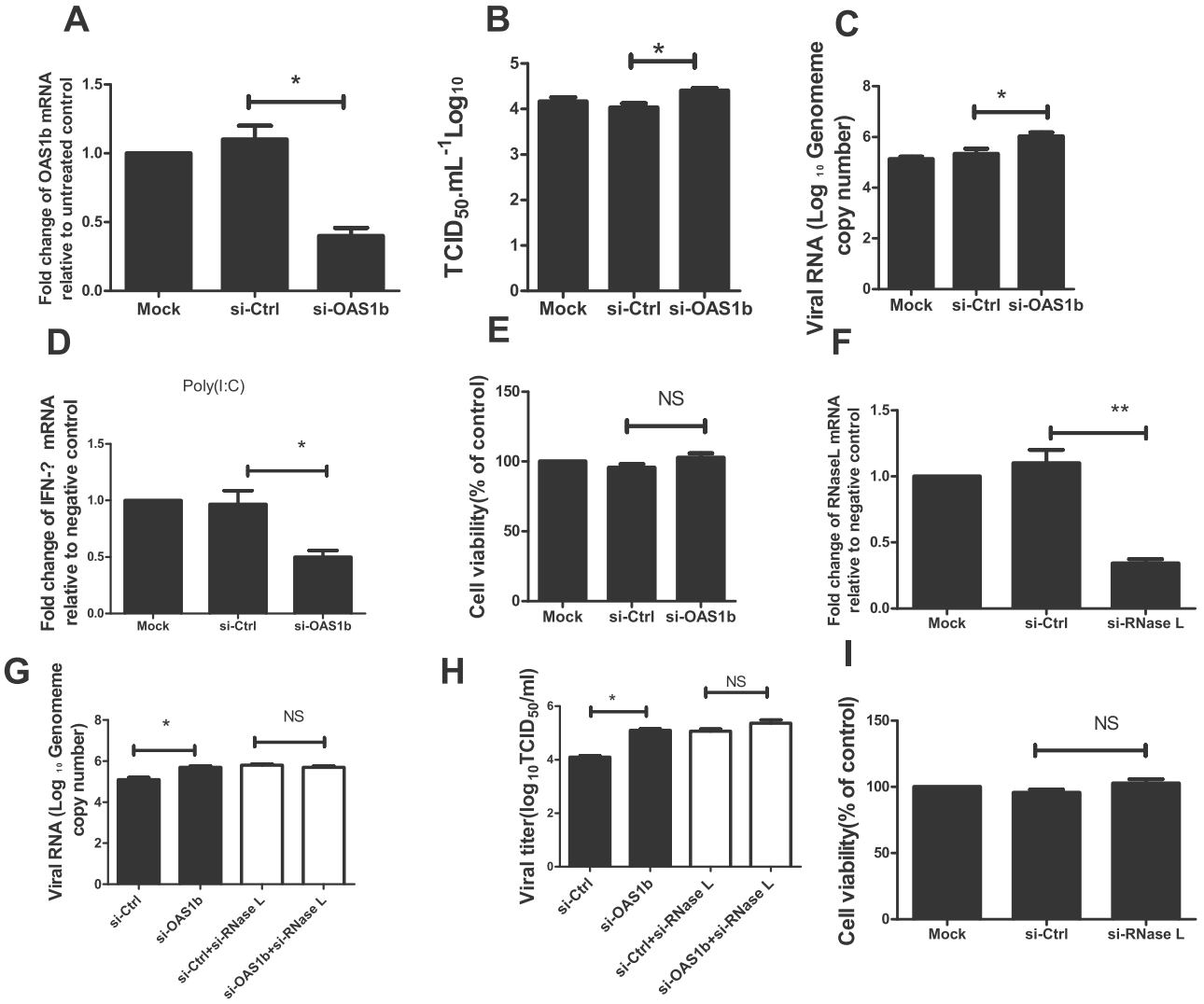

Fig. 5. *OAS1b* silencing via RNA interference promotes viral replication, and the antiviral effect is dependent on RNase L. (A) qPCR measurement of *OAS1b* mRNA expression levels in PAMs transfected with 60 nM si-OAS1b. (B) The virus titer in the culture supernatant of si-OAS1b-transfected PAMs, expressed as $TCID_{50}$. (C) qPCR determination of PRRSV N mRNA expression changes. (D) qPCR analysis of IFN-β expression in si-OAS1b–transfected PAMs. (E) Viability of PAMs transfected with si-OAS1b. (F) qPCR measurement of RNase L mRNA expression in 60 nM si-RNaseL–transfected PAMs. (G) qPCR measurement of PRRSV N mRNA expression in PAMs cotransfected with 60 nM si-RNaseL and 60 nM si-OAS1b and then infected with PRRSV at MOI 0.1. (H) The PRRSV titer in the supernatants of the cultures, expressed as $TCID_{50}$. (I) Viability of PAMs transfected with si-RNaseL.

analysis indicate that the protein contains nucleotidyl transferase (NTase) and OAS domains, with no deletions or mutations in the D-box domain, suggesting that the antiviral activity of this protein may be dependent on RNase L. The follow-up tests confirmed this notion. Nonetheless, no UBL domain was found in pOAS1b, implying that the protein may not be able to interact with RIG-I (Zhu et al., 2014); this finding was expected because RIG-I is not necessary for the antiviral activity of pOAS1b according to our results.

After infection with PRRSV, the highest upregulation of OAS1a was eightfold, and eightfold for OAS1b, while it was sixfold for OASL (data not shown). In addition, during the IFN-β treatment, the highest up-regulation of OAS1a was 400-fold, for OAS1b 500-fold, and for OASL 90-fold (data not shown). The time points at which the three OASs appear to undergo the highest expression are similar, the levels are different, and may be related to the intracellular regulatory pathway governing all three. The three antiviral activities are different too, and the specific mechanisms of action need verification. PRRSV infection also increases pOAS1b expression in different pig organs, especially in the liver (about eightfold) (data not shown), this is same as that of pOASL for classic swine fever virus (Li et al., 2017b).

Two types of cells were tested in this study. The advantage of PAMs is that they can represent the most direct immune response in pigs. The disadvantage is poor transfection efficiency. Only small RNAs such as siRNA or Poly(I:C) can be transfected. Overexpression of plasmids is difficult to implement. CRL-2843-CD163 is a cell line created by passaging PAMs (Wang et al., 2013). The advantage is that it can be more easily transfected with plasmids and thus make up for the defects of PAMs. The disadvantage is that CRL-2843-CD163 cells have gone through artificial transformation (immortalization).

It was recently found that the human *OAS1B* gene confers resistance against infection with the West Nile virus and other flaviviruses (e.g., dengue fever virus, yellow fever virus, and Japanese encephalitis virus) (Ferguson et al., 2008; Kajaste-Rudnitski et al., 2006; Lucas et al., 2003; Mashimo et al., 2002; Perelygin et al., 2002). According to that study, pig OAS1b inhibits Japanese encephalitis virus. In terms of suppression efficiency, pig OAS1b was found to be more effective against PRRSV. This result may be attributable to differences in the characteristics of viruses and cell lines.

In conclusion, all of three porcine OAS which are an anti-PRRSV ISG seems to be effective at inhibiting the replication of PRRSV, they active

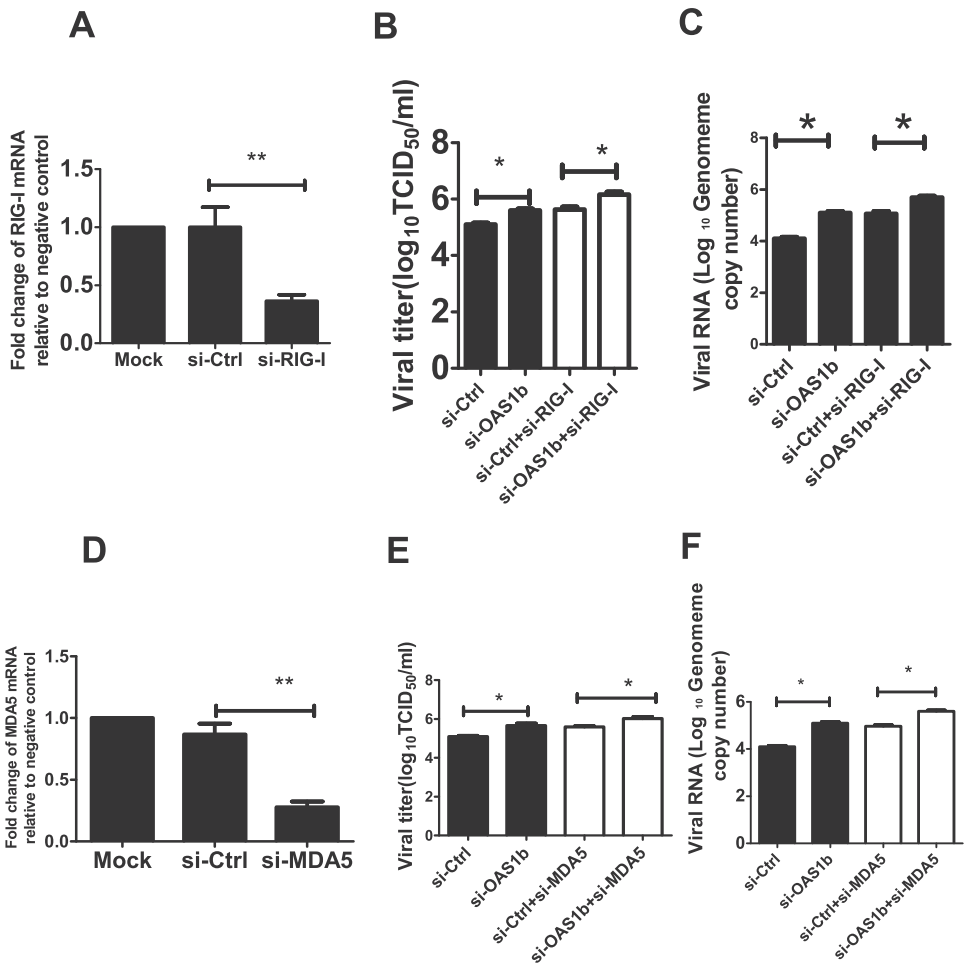

Fig. 6. The antiviral effect is not dependent on RIG-I and MDA5. (A) qPCR measurement of *RIG-I* mRNA expression in PAMs transfected with 60 nM si-RIG-I. (B) The virus titer, expressed as $TCID_{50}$, in PAMs cotransfected with 60 nM si-RIG-I and 60 nM si-OAS1b and then infected 24 h later with PRRSV (MOI 0.1). The virus $TCID_{50}$ was determined in MARC-145 cells. (C) qPCR measurement of PRRSV N mRNA expression in PAMs cotransfected with 60 nM si-RIG-I and 60 nM si-OAS1b and then infected with PRRSV (MOI 0.1) 24 h later. (D) qPCR analysis of *MDA5* mRNA expression in PAMs transfected with 60 nM si-MDA5. (E) The virus titer in PAMs cotransfected with 60 nM si-RIG-I and 60 nM si-MDA5 and then infected with PRRSV (MOI 0.1) 24 h later. The virus $TCID_{50}$ was determined in Marc-145 cells. (F) qPCR measurement of PRRSV N mRNA expression in PAMs cotransfected with 60 nM si-RIG-I and 60 nM si-OAS1b and then infected with PRRSV (MOI 0.1) 24 h later.

the type I IFN-signaling pathway. Upregulation of OAS expression and activity may boost host immunity to limit viral infection. Thus, future investigation of OAS expression might provide the insight and opportunities needed for therapeutic development.

Conflict of interest

The authors declare that they have no conflicts of interest.

Acknowledgements

This work was funded by the Scientific Research Foundation of the Programs for Science and Technology Development of Henan Province, China (grant No. 162102110033 and 182102110083), the Doctoral Startup Fund for Henan University of Animal Husbandry and Economy and research and innovation team of Henan University of Animal Husbandry and Economy (2018KYTD18).

Appendix A. Supplementary data

Supplementary material related to this article can be found, in the online version, at doi:https://doi.org/10.1016/j.vetimm.2019.01.003.

References

Benfield, D.A., Nelson, E., Collins, J.E., Harris, L., Goyal, S.M., Robison, D., Christianson, W.T., Morrison, R.B., Gorcyca, D., Chladek, D., 1992. Characterization of swine infertility and respiratory syndrome (SIRS) virus (isolate ATCC VR-2332). J. Vet. Diagn. Invest. 4, 127–133.

Cagliani, R., Fumagalli, M., Guerini, F.R., Riva, S., Galimberti, D., Comi, G.P., Agliardi, C., Scarpini, E., Pozzoli, U., Forni, D., Caputo, D., Asselta, R., Biasin, M., Paraboschi, E.M., Bresolin, N., Clerici, M., Sironi, M., 2012. Identification of a new susceptibility variant for multiple sclerosis in OAS1 by population genetics analysis. Hum. Genet. 131, 87–97.

Castelli, J.C., Hassel, B.A., Maran, A., Paranjape, J., Hewitt, J.A., Li, X.L., Hsu, Y.T., Silverman, R.H., Youle, R.J., 1998. The role of 2'-5' oligoadenylate-activated ribonuclease L in apoptosis. Cell Death Differ. 5, 313–320.

Cavanagh, D., 1997. Nidovirales: a new order comprising Coronaviridae and Arteriviridae. Arch. Virol. 142, 629–633.

Chebath, J., Benech, P., Revel, M., Vigneron, M., 1987. Constitutive expression of (2'-5') oligo A synthetase confers resistance to picornavirus infection. Nature 330, 587–588.

Dong, B., Silverman, R.H., 1997. A bipartite model of 2-5A-dependent RNase L. J. Biol. Chem. 272, 22236–22242.

Eskildsen, S., Justesen, J., Schierup, M.H., Hartmann, R., 2003. Characterization of the 2'-5'-oligoadenylate synthetase ubiquitin-like family. Nucleic Acids Res. 31, 3166–3173.

Ferguson, W., Dvora, S., Gallo, J., Orth, A., Boissinot, S., 2008. Long-term balancing selection at the west nile virus resistance gene, Oas1b, maintains transspecific polymorphisms in the house mouse. Mol. Biol. Evol. 25, 1609–1618.

Fu, B., Zhao, M., Wang, L., Patil, G., Smith, J.A., Juncadella, I.J., Zuvela-Jelaska, L., Dorf, M.E., Li, S., 2017. RNAi screen and proteomics reveal NXF1 as a novel regulator of IRF5 signaling. Sci. Rep. 7, 2683.

Hartmann, R., Olsen, H.S., Widder, S., Jorgensen, R., Justesen, J., 1998. p59OASL, a 2'-5' oligoadenylate synthetase like protein: a novel human gene related to the 2'-5' oligoadenylate synthetase family. Nucleic Acids Res. 26, 4121–4128.

Hartmann, R., Justesen, J., Sarkar, S.N., Sen, G.C., Yee, V.C., 2003. Crystal structure of the 2'-specific and double-stranded RNA-activated interferon-induced antiviral protein 2'-5'-oligoadenylate synthetase. Mol. Cell 12, 1173–1185.

Hovanessian, A.G., 2007. On the discovery of interferon-inducible, double-stranded RNA activated enzymes: the 2'-5'oligoadenylate synthetases and the protein kinase PKR. Cytokine Growth Factor Rev. 18, 351–361.

Hovanessian, A.G., Justesen, J., 2007. The human 2'-5'oligoadenylate synthetase family: unique interferon-inducible enzymes catalyzing 2'-5' instead of 3'-5' phosphodiester bond formation. Biochimie 89, 779–788.

Hovanessian, A.G., Kerr, I.M., 1979. The (2'-5') oligoadenylate (pppA2'-5'A2'-5'A) synthetase and protein kinase(s) from interferon-treated cells. Eur. J. Biochem. / FEBS 93, 515–526.

Kajaste-Rudnitski, A., Mashimo, T., Frenkiel, M.P., Guenet, J.L., Lucas, M., Despres, P., 2006. The 2',5'-oligoadenylate synthetase 1b is a potent inhibitor of West Nile virus replication inside infected cells. J. Biol. Chem. 281, 4624–4637.

Kakuta, S., Shibata, S., Iwakura, Y., 2002. Genomic structure of the mouse 2',5'-oligoadenylate synthetase gene family. J. Interferon Cytokine Res. 22, 981–993.
Kim, H.S., Kwang, J., Yoon, I.J., Joo, H.S., Frey, M.L., 1993. Enhanced replication of porcine reproductive and respiratory syndrome (PRRS) virus in a homogeneous subpopulation of MA-104 cell line. Arch. Virol. 133, 477–483.
Li, H., Chen, X., Zhao, M., Zhou, e., Qiao, S., Zhang, g., 2017a. Analysis of related molecular changes of innate immune signaling pathway in porcine reproductive and respiratory syndrome virus infected PAMs. Acta veterinaria et Zootechnica Sinic 48, 1288–1299.
Li, L.F., Yu, J., Zhang, Y., Yang, Q., Li, Y., Zhang, L., Wang, J., Li, S., Luo, Y., Sun, Y., Qiu, H.J., 2017b. Interferon-inducible oligoadenylate synthetase-like protein acts as an antiviral effector against classical swine fever virus via the MDA5-mediated type I interferon-signaling pathway. J. Virol. 91.
Lucas, M., Mashimo, T., Frenkiel, M.P., Simon-Chazottes, D., Montagutelli, X., Ceccaldi, P.E., Guenet, J.L., Despres, P., 2003. Infection of mouse neurones by West Nile virus is modulated by the interferon-inducible 2'-5' oligoadenylate synthetase 1b protein. Immunol. Cell Biol. 81, 230–236.
Mashimo, T., Lucas, M., Simon-Chazottes, D., Frenkiel, M.P., Montagutelli, X., Ceccaldi, P.E., Deubel, V., Guenet, J.L., Despres, P., 2002. A nonsense mutation in the gene encoding 2'-5'-oligoadenylate synthetase/L1 isoform is associated with West Nile virus susceptibility in laboratory mice. Proc. Natl. Acad. Sci. U. S. A. 99, 11311–11316.
Patil, G., Zhao, M., Song, K., Hao, W., Bouchereau, D., Wang, L., Li, S., 2018. TRIM41-mediated ubiquitination of nucleoprotein limits influenza a virus infection. J. Virol. 92 (Aug. (16)) e00905-18.
Perelygin, A.A., Scherbik, S.V., Zhulin, I.B., Stockman, B.M., Li, Y., Brinton, M.A., 2002. Positional cloning of the murine flavivirus resistance gene. Proc. Natl. Acad. Sci. U. S. A. 99, 9322–9327.
Schoggins, J.W., Wilson, S.J., Panis, M., Murphy, M.Y., Jones, C.T., Bieniasz, P., Rice, C.M., 2015. A diverse range of gene products are effectors of the type I interferon antiviral response. Nature 525, 144.
Shimizu, N., Sokawa, Y., 1983. (2'-5')Oligoadenylate synthetase in pig spleen: isolation and characterization. J. Biochem. 94, 1421–1428.
Sokawa, J., Sokawa, Y., 1986. (2'-5') oligoadenylate synthetase in chicken embryo erythrocytes and immature red blood cells. J. Biochem. 99, 119–124.
Tessier, M.C., Qu, H.Q., Frechette, R., Bacot, F., Grabs, R., Taback, S.P., Lawson, M.L., Kirsch, S.E., Hudson, T.J., Polychronakos, C., 2006. Type 1 diabetes and the OAS gene cluster: association with splicing polymorphism or haplotype? J. Med. Genet. 43, 129–132.
Tian, K., Yu, X., Zhao, T., Feng, Y., Cao, Z., Wang, C., Hu, Y., Chen, X., Hu, D., Tian, X., Liu, D., Zhang, S., Deng, X., Ding, Y., Yang, L., Zhang, Y., Xiao, H., Qiao, M., Wang, B., Hou, L., Wang, X., Yang, X., Kang, L., Sun, M., Jin, P., Wang, S., Kitamura, Y., Yan, J., Gao, G.F., 2007. Emergence of fatal PRRSV variants: unparalleled outbreaks of atypical PRRS in China and molecular dissection of the unique hallmark. PLoS One 2, e526.
Triozzi, P.L., Avery, K.B., Abou-Issa, H.M., Chou, T.C., 1989. Combined effects of interferon and steroid hormones on 2',5'-oligoadenylate synthetase activity in chronic lymphocytic leukemia cells. Leuk. Res. 13, 437–443.
Wang, X., Ruifang, W., Shuqi, X., Enmin, Z., 2013. Generation of a porcine alveolar macrophage cell line stably expressing CD163 by lentiviral vector for the production of porcine reproductive and respiratory syndrome virus. Acta veterinaria et zootechnica sinic 44, 1797–1804.
Wang, H., Bai, J., Fan, B., Li, Y., Zhang, Q., Jiang, P., 2016. The interferon-induced Mx2 inhibits porcine reproductive and respiratory syndrome virus replication. J. Interferon Cytokine Res. 36, 129–139.
Wang, R., Ma, H., Kang, Y., Li, C., Li, H., Zhang, E., Ji, P., He, J., Zhao, M., 2018a. Molecular cloning and identification of the 2'-5' oligoadenylate synthetase 2 gene in Chinese domestic pigs through bioinformatics analysis, and determination of its antiviral activity against porcine reproductive and respiratory syndrome virus infection. Indian J. Microbiol. 58, 332–344.
Wang, R., Yu, Y., Kong, W., Li, C., Kang, Y., Wang, G., Wang, W., He, J., Zhao, M., 2018b. Molecular cloning of porcine 2',5'-oligoadenylate synthetase-like protein and its role in porcine reproductive and respiratory syndrome virus infection. Microb. Pathog. 125, 281–289.
Yang, C., Liu, F., Chen, S., Wang, M., Jia, R., Zhu, D., Liu, M., Sun, K., Yang, Q., Wu, Y., Chen, X., Cheng, A., 2016. Identification of 2'-5'-oligoadenylate synthetase-like gene in goose: gene structure, expression patterns, and antiviral activity against newcastle disease virus. J. Interferon Cytokine Res. 36, 563–572.
Zhao, M., Ning, Z., Wang, H., Huang, Z., Zhang, M., Zhang, G., 2013. Sequence analysis of NSP9 gene of 25 PRRSV strains from Guangdong province, subtropical southern China. Virus Genes 46, 88–96.
Zhao, J., Feng, N., Li, Z., Wang, P., Qi, Z., Liang, W., Zhou, X., Xu, X., Liu, B., 2016a. 2',5'-Oligoadenylate synthetase 1(OAS1) inhibits PRRSV replication in Marc-145 cells. Antiviral Res. 132, 268–273.
Zhao, M., Qian, J., Xie, J., Cui, T., Feng, S., Wang, G., Wang, R., Zhang, G., 2016b. Characterization of polyclonal antibodies against nonstructural protein 9 from the porcine reproductive and respiratory syndrome virus. Front. Agric. Sci. Eng. 3, 153–160.
Zhao, M., Wan, B., Li, H., He, J., Chen, X., Wang, L., Wang, Y., Xie, S., Qiao, S., Zhang, G., 2017a. Porcine 2', 5'-oligoadenylate synthetase 2 inhibits porcine reproductive and respiratory syndrome virus replication in vitro. Microb. Pathog. 111, 14–21.
Zhao, M., Wang, L., Li, S., 2017b. Influenza a virus-host protein interactions control viral pathogenesis. Int. J. Mol. Sci. 18.
Zhou, L., Wang, Z., Ding, Y., Ge, X., Guo, X., Yang, H., 2015. NADC30-like strain of porcine reproductive and respiratory syndrome virus, China. Emerging Infect. Dis. 21, 2256–2257.
Zhu, J., Zhang, Y., Ghosh, A., Cuevas, R.A., Forero, A., Dhar, J., Ibsen, M.S., Schmid-Burgk, J.L., Schmidt, T., Ganapathiraju, M.K., Fujita, T., Hartmann, R., Barik, S., Hornung, V., Coyne, C.B., Sarkar, S.N., 2014. Antiviral activity of human OASL protein is mediated by enhancing signaling of the RIG-I RNA sensor. Immunity 40, 936–948.